MNRAS 000, 1–10 (2016) Preprint 23 September 2016 Compiled using MNRAS LATEX style file v3.0

# Not a Copernican observer: biased peculiar velocity statistics in the local Universe

Wojciech A. Hellwing[1,2⋆], Adi Nusser[3], Martin Feix[4] and Maciej Bilicki[5,2]
[1]Institute of Cosmology and Gravitation, University of Portsmouth, Portsmouth PO1 3FX, UK
[2]Janusz Gil Institute of Astronomy, University of Zielona Góra, ul. Szafrana 2, 65-516 Zielona Góra, Poland
[3]Department of Physics and the Asher Space Research Institute, Israel Institute of Technology Technion, Haifa 32000, Israel
[4]CNRS, UMR 7095 & UPMC, Institut dAstrophysique de Paris, 98 bis Boulevard Arago, 75014 Paris, France
[5]Sterrewacht Leiden, Universiteit Leiden, Niels Borhweg 2, NL-2333 CA Leiden, the Netherlands

arXiv:1609.07120v1 [astro-ph.CO] 22 Sep 2016

Accepted XXXXXX. Received XXXXXX; in original form XXXXXX

**ABSTRACT**

We assess the effect of the local large scale structure on the estimation of two-point statistics of the observed radial peculiar velocities of galaxies. A large N-body simulation is used to examine these statistics from the perspective of random observers as well as "Local Group (LG)-like" observers conditioned to reside in an environment resembling the observed universe within 20 Mpc. The local environment systematically distorts the shape and amplitude of velocity statistics with respect to ensemble-averaged measurements made by a Copernican (random) observer. The Virgo cluster has the most significant impact, introducing large systematic deviations in all the statistics. For a simple "top-hat" selection function, an idealized survey extending to $\sim 160h^{-1}\,\mathrm{Mpc}$ or deeper is needed to completely mitigate the effects of the local environment. Using shallower catalogues leads to systematic deviations of the order of 50 to 200% depending on the scale considered. For a flat redshift distribution similar to the one of the CosmicFlows-3 survey, the deviations are even more prominent in both the shape and amplitude at all separations considered ($\lesssim 100h^{-1}\,\mathrm{Mpc}$). Conclusions based on statistics calculated without taking into account the impact of the local environment should be revisited.

**Key words:** galaxies: haloes - cosmology: theory, dark matter

## 1 INTRODUCTION

A pillar of cosmology is the Cosmological Principle (Milne 1935) stating that the Universe approaches isotropy and homogeneity with increasing scales[1]. This principle is incorporated in the modern hierarchical scenario for structure formation, where matter density fluctuations are well defined, with a correlation function approaching zero on large scales. In such a scenario, initial fluctuations are described by homogeneous Gaussian random fields, and thus measurements made by different random observers are equivalent. The difference in the statistical properties inferred by these observers is commonly denoted as "cosmic variance". Assuming that our position in the Universe is not privileged, which is expressed in terms of the Copernican Principle (e.g. Uzan 2009), deep large-scale galaxy redshift surveys (*e.g.* Colless et al. 2001; Tegmark et al. 2004; Scrimgeour et al. 2012; Sánchez et al. 2012; Nadathur 2013; Guzzo et al. 2014; Alpaslan et al. 2014) as well as detailed analyses of the cosmic microwave background radiation (Hinshaw et al. 2013; The Planck Collaboration et al. 2013; Planck Collaboration et al. 2015) broadly support this picture.

Recent years have witnessed the advent of high-quality and rich galaxy peculiar velocity data, *e.g.* the SFI++ (Springob et al. 2007), 6dF (Springob et al. 2014), and CosmicFlows catalogues (Courtois et al. 2011; Tully et al. 2013, 2016). This re-kindled activity in the peculiar velocity field with the new data offering an unprecedented opportunity for cosmological measurements and theory testing. In late-time linear theory, peculiar velocities are proportional to the gravitational force field. Therefore, peculiar velocity catalogues are a direct probe of dark matter and can in principle provide valuable information on fundamental theories for structure formation Strauss & Willick (1995).

Inference of cosmological information from local observations must take into account the uncertainties introduced by cosmic variance. This has been known for a long time, dating back to early studies of the density field of galaxies (*e.g.* Sandage 1978; Huchra et al. 1983; Soifer et al. 1984; Geller & Huchra 1989). While cosmic variance in the statistical analysis of the galaxy distribution is well studied, its implications on peculiar velocity observations have received little attention (but see Tormen et al. 1993; Strauss et al. 1998; Bilicki & Chodorowski 2010; Hellwing 2014) and remain poorly understood. Due to the long-range nature of gravity,

⋆ E-mail: pchela@icm.edu.pl

[1] A counter example to the Cosmological Principle is a distribution of particles in a random fractal encompassing empty volumes of the same size as the whole probed region (Peebles 1980; Nusser & Lahav 2000)

© 2016 The Authors

local structures affect velocity correlations on much larger scales than those relevant to the density field (Tormen et al. 1993; Borgani et al. 2000; Chodorowski & Ciecielag 2002). With reliable velocity catalogues only available for galaxies out to distances of 100–200 $h^{-1}\,\mathrm{Mpc}$, the impact of nearby structures is likely very significant. A similar effect was already hinted for the case of a local velocity field dispersion measure (Cooray & Caldwell 2006; Marra et al. 2013; Wojtak et al. 2014).

Galaxy peculiar velocities are practically unbiased with respect to the underlying velocity field (*e.g.* Vittorio et al. 1986; Górski 1988; Groth et al. 1989; Strauss & Willick 1995; Nusser & Colberg 1998; Feldman et al. 2003a; Juszkiewicz et al. 2000; Sarkar et al. 2007; Nusser et al. 2011; Hudson & Turnbull 2012; Nusser et al. 2012; Feix et al. 2015). This is in contrast to the galaxy distribution in redshift surveys which is a biased tracer of the mass density field. Thus, peculiar velocity catalogues are not merely complementary to redshift-space distortions, but provide an independent avenue towards testing fundamental physical theories of structure formation, dynamical dark energy and modified gravity (Zu et al. 2013; Li et al. 2013; Hellwing et al. 2014; Berti et al. 2015; Bull 2016).

Extracting cosmological information from the observed motions is, however, a highly non-trivial matter. Despite the recent increase in quality and number of distance indicator measurements, the corresponding peculiar velocity catalogues remain relatively sparse with significant observational and systematic errors especially at larger distances. There are several approaches for inferring cosmological information from the observations. One could make an attempt at reconstructing a 3D peculiar velocity field from which the underlying mass density can be derived. This would be very rewarding but the effort is hampered by the notorious inhomogeneous Malmquist bias (Lynden-Bell et al. 1988a,b) leading to spurious enhancement of the derived density fluctuations. A more straightforward strategy which has provided important constraints on the standard paradigm is to compare between the measured velocities and the gravitational field associated with an independent redshift survey (see *e.g.* Davis et al. 2011). Although this analysis is free from cosmic variance uncertainties and is mainly free from Malmquist biases, it relies on redshift surveys and is therefore dependent on the biasing relation between mass and galaxies.

Our main goal in this paper is to systematically assess the impact of cosmic variance and observer location on the peculiar velocity observables such as velocity correlation functions and mean streaming velocities (the first moment of galaxy pairwise velocity distribution).

We neglect meagre redshift evolution which might be present in local ($z \approx 0$) peculiar velocity catalogues. Further, we make no attempt at incorporating observational errors on the measured velocities. These errors increase with distance and can obviously lead to large uncertainties. Subsequently, we do not model any inhomogeneous Malmquist bias related to these errors.

This paper is organised as follows: in §2 we describe the numerical assets used in this work; section §3 introduces and describes velocity statistics we consider; in §4 we discuss various theoretical biases, while in §5 we study the impact of observer location and galaxy radial selection on the velocity statistics. We conclude with a general discussion of our results and their implications in §6.

## 2 SIMULATIONS

Ideally we would like to study the velocity field of galaxies themselves. However, realistic modelling of galaxy formation physics in a computer simulation is very difficult and computationally challenging. Hence we will use here DM haloes and their peculiar velocities as proxies for luminous galaxies. In principle, such approach could hinder our analysis by introducing systematic biases reflecting the fact that we ignore all the complicated baryonic physics. Energetic feedback processes such as Active Galactic Nuclei, star formation together with dynamical gas friction and ram pressure striping could significantly affect the velocities of visible (stellar) components of galaxies with respect to their DM halo hosts. However, recently Hellwing et al. (2016) using EAGLE, the state-of-the-art galaxy formation simulation (Schaye et al. 2015), have shown that peculiar velocities of galaxies inhabiting haloes with $M_{200} > 2 \times 10^{11} h^{-1}\mathrm{M}_{\odot}$ are on average affected by the baryonic effects at the level of at most 1 km/s, while even smaller (dimmer) galaxies are affected at the level of at most a $10 - 20$ km/s. For all our practical purposes such small effects would have negligible impact on our analysis, indicating that we can safely ignore baryonic effects and model the galaxy peculiar velocity field using DM haloes as their proxies.

We will base our analysis on a new $\Lambda$CDM N-body simulation dubbed "Warsaw Universe". The detailed description of this resource will be presented in an accompanying paper (Hellwing in prep.). Here we will limit ourselves to presenting only the most important aspects of this simulation relevant for our study. The simulation consists of 2 billion DM particles ($1280^3$) placed in a uniform cube of $800h^{-1}\,\mathrm{Mpc}$ width. It was evolved using publicly available GADGET2 code (Springel 2005). The initial conditions were set at $z = 63$ using the Zel'dovich approximation (Zel'Dovich 1970). The initial density fluctuations power spectrum was chosen to follow WMAP7 best-fit values of cosmological parameters (Komatsu & et al. 2010, data wmap7+bao+h0): $\Omega_0 h^2 = 0.134, \Omega_b h^2 = 0.0226, \Omega_\lambda = 0.728, \sigma_8 = 0.809, n_s = 0.963, h = 0.704$. In this work only the final snapshot of the simulation ($z = 0$) will be considered, as we are interested in the local galaxy velocity field. Thus, the resulting resolutions of the simulation are: $m_p = 1.84 \times 10^{10} h^{-1}\mathrm{M}_{\odot}$ for the mass and $\varepsilon = 20h^{-1}\,\mathrm{kpc}$ for the force.

DM haloes have been identified by means of the phase-space Friends-of-Friends ROCKSTAR halo finder, kindly provided to the public by Behroozi et al. (2013). For the $z = 0$ simulation output, ROCKSTAR gave a little more than $\sim 5.5 \times 10^6$ bound DM haloes with a minimum of 20 particles per halo (*i.e.*with minimum $M_{200} = 3.7 \times 10^{11} h^{-1}\mathrm{M}_{\odot}$). Here we define the halo mass as $M_{200} = 4/3\pi R_{200}^3 200 \times \rho_c$, where the radius $R_{200}$ is the distance from a halo centre enclosing a sphere with an average density of $200\rho_c$ where $\rho_c = 3H^2/8\pi G$ is the critical density. The bulk velocity of each halo is taken as the velocity vector of its centre-of-mass. In the analysis of distance indicator catalogues, galaxies in groups and clusters are usually grouped together. To match that we have excised satellite subhaloes from our halo catalogue.

## 3 VELOCITY STATISTICS

In this section we will describe two velocity statistics that are our primary focus in this work. Namely the velocity correlation functions and moments of pairwise velocity distribution function. In principle the cosmological information is encoded in the full three

dimensional velocity field of galaxies. However, this is not accessible by astronomical observations, with a few exceptions in the very local Universe (Local Group) [2]. Hence we need to limit ourselves to only the radial component of the peculiar velocity field, which is a projection of the full 3D velocity vectors onto the line of sight connecting an observer with an object in question.

We set the scale factor, $a$, to unity at the present time and denote the corresponding Hubble constant with $H_0$. The peculiar velocity of a test particle is $\dot{\mathbf{x}}$ where $\mathbf{x}$ is the comoving position of the particle. The density contrast is $\delta(\mathbf{x}) = \rho(\mathbf{x})/\bar{\rho} - 1$ where $\rho(\mathbf{x})$ is the local density and $\bar{\rho}$ is the mean background density.

### 3.1 Velocity Correlation Functions

The correlation properties of a 3D peculiar velocity field, $\mathbf{v}(\mathbf{x})$, are specified by the velocity correlation tensor

$$\Psi_{ij}(\mathbf{r}) \equiv \langle v_i(\mathbf{x}) v_j(\mathbf{x}+\mathbf{r}) \rangle \ , \tag{1}$$

where $i, j$ are Cartesian components of $\mathbf{v}$ and $\mathbf{r}$ is the separation between two points in space. For a statistically homogeneous and isotropic velocity field the velocity correlation tensor can be written as a linear combination of parallel (to the separation vector), $\Psi_\parallel$, and transverse, $\Psi_\perp$, velocity correlation functions (Górski 1988)

$$\Psi_{ij}(r) = \Psi_\perp(r)\delta_{ij} + \left[\Psi_\parallel(r) - \Psi_\perp(r)\right] \hat{r}_i \hat{r}_j \ , \tag{2}$$

where $\delta_{ij}$ is the Kronecker delta.

In linear theory, the velocity correlations can easily be expressed in terms of the power spectrum $P(k)$ of the density fluctuations $\delta(\mathbf{x})$. Linear theory relates the Fourier components of peculiar velocity and density fluctuation fields by (*e.g.* Peebles 1980)

$$\mathbf{v}(\mathbf{k}) = -iH_0 f \frac{\hat{\mathbf{k}}}{k} \delta(\mathbf{k}) \ , \tag{3}$$

where $f \equiv \mathrm{d}\ln D_+(a)/\mathrm{d}\ln a$ is the growth rate of density perturbations. This yields (Górski 1988):

$$\Psi_\perp(r) = \frac{H_0^2 f^2}{2\pi^2} \int P(k) \frac{j_1(kr)}{kr} \mathrm{d}r \, , \tag{4}$$

and

$$\Psi_\parallel(r) = \frac{H_0^2 f^2}{2\pi^2} \int P(k) \left[ \frac{j_0(kr)}{kr} - 2\frac{j_1(kr)}{kr} \right] \mathrm{d}r \, , \tag{5}$$

where

$$j_0(y) = \frac{\sin y}{y} \quad \text{and} \quad j_1(y) = \frac{\sin y}{y^2} - \frac{\cos y}{y} \ . \tag{6}$$

Thus, in principle, measurements of $\Psi_\parallel$ and $\Psi_\perp$ should provide constraints on a combination of the cosmological power spectrum and the growth rate, independent of galaxy biasing.

#### 3.1.1 *Correlations from radial velocities*

Observations provide access to the radial (line of sight) components of the galaxy peculiar velocities. Hence the transverse and parallel correlation functions cannot be measured directly. Górski et al. (1989) and Groth et al. (1989) proposed alternative velocity correlation statistics which could readily be computed from the observed radial components. Given a sample of $N$ galaxies with positions $\mathbf{r}_\alpha$ and radial peculiar velocities $u_\alpha = \mathbf{v}_\alpha \cdot \hat{\mathbf{r}}_\alpha$ ($\alpha = 1 \cdots N$), let the separation vector between two galaxies be $\mathbf{r} = \mathbf{r}_\alpha - \mathbf{r}_\beta$, and the corresponding subtended angles are $\cos\theta_{\alpha\beta} = \hat{\mathbf{r}}_\alpha \cdot \hat{\mathbf{r}}_\beta$ and $\cos\theta_\alpha = \hat{\mathbf{r}} \cdot \hat{\mathbf{r}}_\alpha$. Then these statistics are defined as (Górski et al. 1989)

$$\psi_1(r) = \frac{\sum_{\alpha,\beta} u_\alpha u_\beta \cos\theta_{\alpha\beta}}{\sum_{\alpha,\beta} \cos^2\theta_{\alpha\beta}} \, , \tag{7}$$

and

$$\psi_2(r) = \frac{\sum_{\alpha,\beta} u_\alpha u_\beta \cos\theta_\alpha \cos\theta_\beta}{\sum_{\alpha,\beta} \cos\theta_{\alpha\beta} \cos\theta_\alpha \cos\theta_\beta} \, , \tag{8}$$

where the summation covers all galaxy pairs with separation $r < |\mathbf{r}_\alpha - \mathbf{r}_\beta| < r + \Delta r$. The ensemble average of either of $\psi_{1,2}(r)$ is a linear combination of $\Psi_\perp(r)$ and $\Psi_\parallel(r)$,

$$\Psi_{1,2}(r) \equiv \langle \psi_{1,2}(r) \rangle = X_{1,2}(r)\Psi_\parallel(r) + [1 - X_{1,2}(r)]\, \Psi_\perp(r) \, , \tag{9}$$

where the geometrical factors $X_{1,2}$ can be estimated directly from the data

$$X_1(r) = \frac{\sum_{\alpha,\beta} \left[\mathbf{r}_\alpha \mathbf{r}_\beta (\cos^2\theta_{\alpha\beta} - 1) + r^2 \cos\theta_{\alpha\beta}\right] \cos\theta_{\alpha\beta}}{r^2 \sum_{\alpha,\beta} \cos^2\theta_{\alpha\beta}} \, , \tag{10}$$

$$X_2(r) = \frac{\sum_{\alpha,\beta} \left[\mathbf{r}_\alpha \mathbf{r}_\beta \left(\cos^2\theta_{\alpha\beta} - 1\right) + r^2 \cos^\beta \theta_{\alpha\beta}\right]^2}{r^2 \sum_{\alpha,\beta} \left[\mathbf{r}_\alpha \mathbf{r}_2 \left(\cos^2\theta_{\alpha\beta} - 1\right) + r^2 \cos^2\theta_{\alpha\beta}\right] \cos\theta_{\alpha\beta}} \, , \tag{11}$$

The prescription for deriving the continuous limit of these expressions is to replace the summation over particles with integration over space as follows

$$\sum_\alpha (\cdots) \to \int d^3\mathbf{r}_\alpha n_{\rm obs}(\mathbf{r}_\alpha) (\cdots) \ . \tag{12}$$

Here, $n_{\rm obs} = \bar{n}(1+\delta_{\rm g})\phi$ is the observed number density of galaxies and it is the product of the underlying number density $\bar{n}(1+\delta_{\rm g})$ and the selection function imposed on the observations, $\phi$. Since galaxies are biased tracers of mass, the contrast $\delta_{\rm g}$ differs from the mass density contrast $\delta$. Therefore, although the expressions (7) and (8) for $\psi_{1,2}$ are straightforward to compute from a velocity catalogue, the task of inferring cosmological information is quite challenging and difficult.

### 3.2 Pairwise velocity correlation

The other velocity statistics that we consider is the first moment of the galaxy/halo pairwise velocity distribution. It is sometimes dubbed as *pairwise streaming velocity* and indicated as $v_{12}$. This statistic was introduced by Davis & Peebles (1977) in the context of the *Bogoliubov-Born-Green-Kirkwood-Yvon hierarchy* (BBGKY), a kinetic theory which describes the dynamical evolution of a system of particles interacting through gravity. This statistic is of special importance for modelling the correlation function of galaxies in redshift space. Here we will focus on its use as a characteristic of the flow pattern as probed by observed radial motions. We begin with the definition of this function in the fluid limit where we are given the full velocity and density fields. In this idealized situation we write

$$\mathbf{v}_{12}(r) = \langle \mathbf{v}_1 - \mathbf{v}_2 \rangle_\rho = \frac{\langle (\mathbf{v}_1 - \mathbf{v}_2)(1+\delta_1)(1+\delta_2) \rangle}{1 + \xi(r)} \ , \tag{13}$$

where $\mathbf{v}_1$ and $\delta_1 = \rho_1/\langle\rho\rangle - 1$ denote the peculiar velocity and fractional matter density contrast at galaxy/halo position $\mathbf{r}_1$. Further $\xi(r) = \langle \delta_1 \delta_2 \rangle$ is the usual 2-point density correlation function. The $\langle \cdots \rangle_\rho$ denotes a pair-weighted average, which differs

[2] But see Nusser et al. (2012) for near-future prospects of measuring transverse velocities with Gaia.

from the usual spatial averaging by the weighting factor, $\mathcal{W} = \rho_1\rho_2/\langle\rho_1\rho_2\rangle$, which is proportional to the number density of pairs. Isotropy implies that $\mathbf{v}_{12}$ has a vanishing component in the perpendicular direction to the separation $\mathbf{r}$, i.e. $\mathbf{v}_{12} = v_{12}\hat{\mathbf{r}}$

In the stable clustering regime, on scales where the pairwise velocity exactly cancels out the Hubble flow, $v_{12} = -H\mathbf{r}$. The pair conservation equation (Peebles 1980) connects $v_{12}(r)$ to the density correlation function $\xi(r)$. Juszkiewicz et al. (1999) suggested an analytical *ansatz* for Eqn. (13), which turned out to be a reasonably good approximation to results from N-body simulations evolved from initial Gaussian conditions. Their formula reads

$$v_{12} = -\frac{2}{3}H_0 r f\bar{\bar{\xi}}(r)[1+\alpha\bar{\bar{\xi}}(r)], \tag{14}$$

where

$$\bar{\xi}(r) = (3/r^3)\int_0^r \xi(x)x^2dx \equiv \bar{\bar{\xi}}(r)[1+\xi(r)]\ . \tag{15}$$

Here $\alpha$ is a parameter that depends on the logarithmic slope of $\xi(r)$. It is clear that $v_{12}(r)$ is a strong function of $\xi(r)$ and $f$. Because of this some authors have suggested to use $v_{12}(r)$ as a cosmological probe (Feldman et al. 2003b; Juszkiewicz et al. 2000; Hellwing et al. 2014; Ma et al. 2015; Fagernes Ivarsen et al. 2016)

### 3.2.1 *Pairwise correlation from radial velocities*

Using a simple least-square approach, Ferreira et al. (1999) derived an estimator of the mean pairwise velocity applicable to catalogues of observed radial peculiar velocities. It takes the following form:

$$\tilde{v}_{12}(r) = \frac{2\sum_{\alpha,\beta}(u_\alpha - u_\beta)p_{\alpha\beta}}{\sum_{\alpha,\beta}p_{\alpha\beta}^2}\ . \tag{16}$$

Here $p_{\alpha\beta} \equiv \hat{r}\cdot(\hat{\mathbf{r}}_\alpha+\hat{\mathbf{r}}_\beta) = \cos\theta_\alpha+\cos\theta_\beta$. The continuous limit of the expression (16) is obtained from the recipe in (12). Therefore, like $\psi_{1,2}$, this estimator depends on the underlying galaxy distribution as well as the selection criteria.

## 4 ESTIMATOR BIASES FOR RANDOMLY SELECTED OBSERVERS

We begin our analysis be assessing how accurately the radial velocity based estimators probe the true underlying 3D quantities. We consider 50 observers randomly placed in the simulation box of $800h^{-1}$ Mpc. We use the full halo catalogue with a minimum halo mass of $3.7\times10^{11}h^{-1}\mathrm{M}_\odot$, and compute the halo radial velocities relative to each observer. Because the radial velocity is observer-dependent, the radial velocity correlations are expected to depend on the location of the observer. We compute the *ensemble* average over all the 50 observers. We treat such an averaged measurement as one made by *the idealized Copernican observer*. This ensemble average is then compared with the correlation function obtained from the full 3D velocity data of the full halo catalogue.

The results are shown in Fig. 1. In the top panel the radial component based estimator of (16) for $v_{12}$ is shown (open symbols) against the result (solid lines) obtained by summing over the same pairs in the simulation but using the full 3D velocity information. We present separately results for DM particles (squares) and haloes (circles), as indicated in the panel. The agreement between the radial velocity and theoretical estimators is superb. For tracers, DM and haloes, and on all considered pair separations up to $100h^{-1}$ Mpc, the differences between the radial component estimator for $v_{12}$ and the values obtained using full 3D information

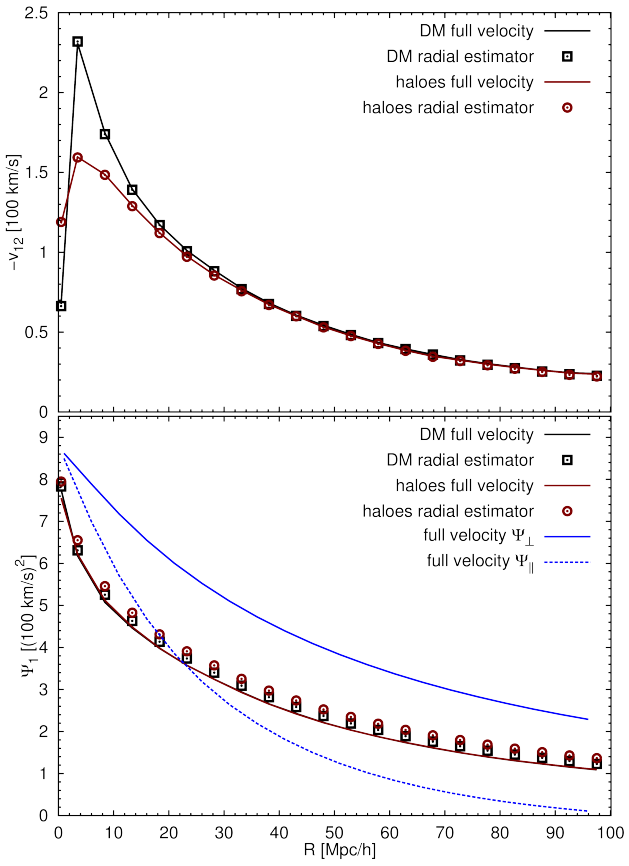


**Figure 1.** The performance of the radial velocity-based estimators compared to statistics extracted using full velocity information. The top panel is for the pairwise velocities $v_{12}$, and the bottom for the velocity correlation function $\psi_1$. In all cases the lines depict results obtained from full 3D velocity information. Open squares and circles correspond to the radial-component based estimators of Eqn. (16) and Eqn. (7) for DM and halo velocities, respectively.

are smaller than $1-2$ km/s. The bottom panel illustrates analogous comparison for $\psi_1$. Because the results for $\psi_2$ follow quantitatively those of $\psi_1$, we omit them for clarity. Since $\psi_1(r)$ is by construction defined only for radial velocities, to get a theoretical prediction to compare with we use Eqn. (9) and Eqn. (11). Here we computed $\Psi_\perp$ and $\Psi_\parallel$ directly from the full 3D velocity field and used them together with the measured geometrical factor $X_1$ to obtain a prediction for $\psi_1$ (which we mark as 'full velocity' lines). Unlike the previous case, the estimators for the velocity correlation functions are slightly biased towards higher values. Although noticeable, the effect is not large. For DM particles it is less than $4\%$ at $R < 20h^{-1}$ Mpc, increasing to $\sim 8\%$ at $60h^{-1}$ Mpc. For haloes, the discrepancy is roughly twice as large. Hence at scales of $60h^{-1}$ Mpc, it can be of the order of $15\%$, which should be taken into account, when one wants to compare $\Psi_\perp$ and $\Psi_\parallel$ derived from measured $\psi_{1,2}$ with theoretical predictions of Eqn. (4) and Eqn. (5).

Having checked that both our radial velocity based estimators preform reasonably well using the full halo catalogue, we now examine effects of the sparse halo sampling. Modern galaxy redshift surveys already contain millions of galaxies, however such a sampling rate is far from the reach of velocity catalogues, consisting of only thousands of objects. Nevertheless, despite the much lower object counts the velocity catalogues retain quite high

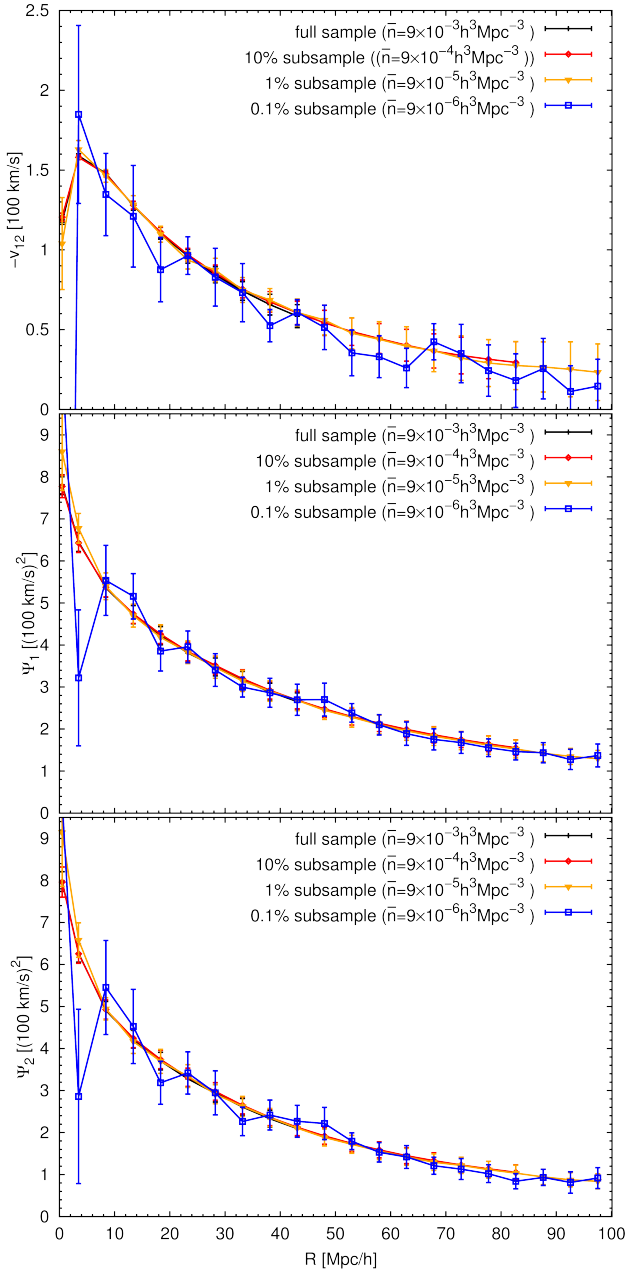


**Figure 2.** Sampling bias for $v_{12}(R)$ (top panel), $\Psi_1(R)$ (middle panel) and $\Psi_2(R)$ (bottom panel). Different lines correspond to different halo samples.

number density of tracers thanks to relatively small and limited volumes that they cover. The currently available velocity catalogues are typically reaching $\bar{n} \approx 10^{-4} - 10^{-5}\,\mathrm{Mpc}^{-3}$. However, such catalogues often need to be further diluted, when one needs to for example reject galaxies with large velocity errors. To assess how our velocity statistics and their estimators are affected by sub-sampling we split our full halo catalogue into three randomly sub-sampled populations. In all the cases, we use the original catalogue and sub-samples containing respectively 10%, 1%, and 0.1% of the full sample. The corresponding spatial abundances of resulting catalogues are: $\bar{n}_{full,10\%,1\%,0.1\%} = 9 \times (10^{-3}, 10^{-4}, 10^{-5}, 10^{-6})h^3\,\mathrm{Mpc}^{-3}$, respectively. The three panels of Fig. 2 illustrate the effect of sparse sampling, from top to bottom for $v_{12}$, $\psi_1$ and $\psi_2$. As previously stated, all the plotted lines are ensemble averages over 50 random observers, with the error bars marking $1\sigma$ dispersions around the ensemble mean. Analysis of the data shown in plots reveals that the sub-sampling only increases the scatter, while averages of both $v_{12}$ and $\psi_{1,2}$ are not affected in any significant way. Only for the case of the most diluted sample with only $1/1000$-th of the original haloes appreciable scatter around the true mean of $v_{12}$ appears. The same subsample traces the averages of $\psi_1$ and $\psi_2$ much better, already at $R \geqslant 20h^{-1}\,\mathrm{Mpc}$ the effects of sparse sampling are small. Furthermore, it is noteworthy that the additional scatter due to sparse sampling is only prominent for small separation bins, indicating that this scatter is sub-dominant to the cosmic variance. Hence we can safely expect that for $R \gtrsim 10h^{-1}\,\mathrm{Mpc}$ the velocity correlation functions are well probed even with samples hundred times scarcer than the complete volume selection sample. These are good news, as we can now expect that relative low sampling rate in the galaxy peculiar velocity surveys should not affect significantly the measured velocity correlations.

## 5 LOCAL GROUP OBSERVERS

So far we have considered random observes in the box. Now we turn to the effects of the nearby large-scale structure on the inferred velocity statistics. We, therefore, aim at selecting LG-analogue observers residing in regions resembling in as much as possible our local environment. The LG is a gravitationally bound system of a dozen major galaxies with the Milky Way (MW) and its neighbouring M31 as the most massive members. The region of 5 Mpc distance from the LG is characterized by moderate density (see *e.g.* Tully & Fisher 1987, 1988; Hudson 1993; Tully et al. 2008; Courtois et al. 2013) and a quiet flow (Sandage et al. 1972; Schlegel et al. 1994; Karachentsev et al. 2002, 2003). Located at a distance of $\sim$ 17 Mpc is the Virgo cluster, whose gravitational effects extend to tens of Mpcs around us, as evident from the corresponding infall flow pattern of galaxies (Tully & Shaya 1984; Tammann & Sandage 1985; Lu et al. 1994; Gudehus 1995; Karachentsev et al. 2014). The presence of such a large non-linear mass aggregation can have a substantial impact on peculiar velocity field of the local galaxies.

To find suitable "observers" in the simulation box we first obtain density and velocity fields on a regular $512^3$ grid by using the publicly available DTFE code (Cautun & van de Weygaert 2011). The DTFE code employs *the Delaunay Tessellation Field Estimation*, a method described in detail in Schaap & van de Weygaert (2000); van de Weygaert & Schaap (2009), which assures that the resulting smooth fields have the highest attainable resolution, are volume weighted and have suppressed sampling noise. The fields are then smoothed using top-hat filtering and the resulting grid cells are used for imposing the local density and velocity constraints. Given the density and velocity fields as well as the halo catalogue we search the simulation for candidate observers. Specifically we demand that "observers" are located in an environment satisfying the following constraints:

(i) the observer is located in a MW-like host halo of mass $7 \times 10^{11} < M_{200}/(h^{-1}\mathrm{M}_\odot) < 2 \times 10^{12}$ (Busha et al. 2011; Phelps et al. 2013; Cautun et al. 2014; Guo et al. 2015),

(ii) the bulk velocity within a sphere of $R = 3.125h^{-1}\,\mathrm{Mpc}$ centred on the observer is $V = 622 \pm 150\,\mathrm{km\,s}^{-1}$ (Kogut et al. 1993),

(iii) the mean density contrast within the same sphere is in the range of $-0.2 \leqslant \delta \leqslant 3$ (Karachentsev et al. 2012; Elyiv et al. 2013; Tully et al. 2014),

(iv) a Virgo-like cluster of mass $M = (1.2\pm0.6)\times10^{15}h^{-1}\mathrm{M}_{\odot}$ is present at a distance $D = 12 \pm 4h^{-1}\,\mathrm{Mpc}$ from the observer (Tammann & Sandage 1985; Mei et al. 2007).

To examine the role of individual criteria we also study results for sets of observers selected without imposing all constraints. The sets of observers we consider are:

**LGO1** is our fiduciary set of 290 observers each satisfying all the selection criteria (i) through (iv).

**LGO2** consists of 1045 candidate observers obtained by relaxing the velocity constraint (ii), but satisfying the remaining criteria.

**LGO3** has 804 candidates obtained by relaxing the density contrast condition (iii) only.

**LGO4** of 1561 candidates with the conditions (ii) & (iii) relaxed simultaneously.

**LGO5** has 1197 observers without imposing the constraint on the host halo mass but with all the other criteria fulfilled.

**LGO–NOV** contains 772543 candidate observers satisfying all conditions except the proximity to a Virgo-like cluster.

**RNDO** is a list of observers with randomly selected positions in the simulation box. This set is used as a benchmark for comparison.

Based on the number of candidate observers in each set, we conclude that the proximity to a Virgo-like cluster is the strongest discriminator among all the conditions. Moreover, positions of observers in each of the 5 sets **LGO1**-**LGO5** are highly correlated, as they are constrained to reside in the same vicinities of Virgo like objects. Therefore, in order to speed up the calculations, we consider only a sub-sample of the list of observes, not reducing however the statistical significance of the results. This is done by laying a uniform coarse $8^3$ grid in the box and selecting, for each set of observers, one random observer per grid cell, should the cell contain any observers. This gives an average number of 60 observers for each of the 5 sets. To match the sample variance we also keep only 64 observers in the **LGO–NOV** and **RNDO** sets. As we have already pointed out, currently available peculiar velocity catalogues are relatively shallow due to the difficulty in measuring distances especially for distant galaxies. Furthermore, additional distance cuts and trimming of the data are usually imposed on velocity catalogues in order to avoid very large errors and uncontrolled observational systematics. To get closer to a realistic catalogue, we implement two simple data weighting schemes. The first scheme mimics simple radial selection cuts that one can always implement for a given peculiar velocity catalogue. It is defined by a single "depth" parameter, $r_w$. Here a halo at a distance $r$ from the observer is assigned a weight, $w_h$, given by

$$w_h = \begin{cases} 1, & \text{if } r \leqslant r_w \\ 0, & \text{otherwise}\,. \end{cases} \tag{17}$$

The second scheme aims at mimicking a sample with a flattened radial distribution of galaxies, similar to the one describing the CosmicFlows-3 catalogue (Tully et al. 2016). Here, the weighting is characterised by a power-law and, in addition to the depth parameter $r_W$, is also a function of the "steepness" parameter $m$. The corresponding formula for $w_h$ is

$$w_h = \begin{cases} 1, & \text{if } r \leqslant r_w \\ (r/r_w)^{-m}, & \text{otherwise}\,. \end{cases} \tag{18}$$

Here we consider $r_w = 20h^{-1}\,\mathrm{Mpc}$ and $m = 2, 3$ and dub the corresponding catalogues *CF3-like m=2* and *CF3-like m=3* accordingly. We will use these data weighting schemes to further investigate how the velocity statistics depend on the catalogue depth.

The three panels to the left in Fig. 3 show the statistics derived for all sets of observers, with $r_w = 80h^{-1}\,\mathrm{Mpc}$ and the first weighting scheme applied. The curves are (ensemble) averages over all observers in each set (as indicated in the figure) and the attached error-bars and filled regions represent the corresponding $1\sigma$ scatter. The error-bars in the **LGO** series are similar and for clarity they are attached only to **LGO1**. Since we do not include observational errors, this scatter is entirely due to cosmic variance among the observers in each set. Plotted also are results for the "Copernican" observer, computed from the full catalogue for the **RNDO** observer set. The small error-bars here reflect the fact that different observers see different (radial) velocity components of the same galaxies. The **LGO** curves in all the panels differ systematically from the Copernican **RNDO** result. However, the **LGO–NOV** and **RNDO** curves are almost indistinguishable up to pair separations of $R \sim 55h^{-1}\,\mathrm{Mpc}$, meaning that the proximity to Virgo is the only significant criterion in the selection of the LG candidate. The average streaming velocity, $v_{12}$, defined in Eqn. (16), in the top-left panel is significantly affected by the LG selection criteria at pair separations $R \gtrsim 40h^{-1}\,\mathrm{Mpc}$. At those scales, LG-observers are deviating from the "Copernican" curve by more than $1\sigma$ getting values lower then the cosmic mean observer. However, the observer-to-observer induced variance is large. So even for smaller scales, where the both averages agree within the scatter, the amplitude of the difference is large and can typically take from 50 to 100 km/s. This is already a $100\%$ level effect at $R = 40h^{-1}\,\mathrm{Mpc}$, but it quickly grows, reaching $200\%$ magnitude difference already at separations of $\sim 60h^{-1}\,\mathrm{Mpc}$. At large separations closer to $r_w$, fewer galaxy/halo pairs are found which explains the rapid increase of the error-bars for LG-observers.

In the middle and bottom-left panels of Fig. 3 we consider the correlation functions, $\psi_1$ and $\psi_2$. For all **LGO** LG-analogues the amplitude of $\psi_1$ is systematically larger than the black curve corresponding to the Copernican observer, up-to separations of $\sim 75h^{-1}\,\mathrm{Mpc}$. At larger separation the sign of the effect is flipped and all **LGO** $\psi_1$'s take smaller amplitudes than a random observer measurement. This is a clear sign of the imposed catalogue depth, with our radial cut of $r_w = 80h^{-1}\,\mathrm{Mpc}$. Here again the observer induced scatter is large making the **LGO** curves to "agree" within $1\sigma$ with the Copernican observer, even though the actual relative difference is typically as large as $\sim 50\%$. However, considering just the small variance of **RNDO**, the **LGO** results would be $> 5\sigma$ away from a cosmic mean. For $\psi_2$ the behaviour is qualitatively similar to the $\psi_1$ case. The main difference consists of a roughly twice smaller scale ($\sim 40h^{-1}\,\mathrm{Mpc}$) at which the flip of the effect's sign occurs. However, the noteworthy feature of $\psi_2$ **LGO** signal is the significantly smaller relative difference from **RNDO**, which typically takes only $25\%$ and also a slightly smaller observer-based variance. Interestingly it seems that also "no Virgo" observers for both $\psi$'s at scales above the "flip off" differ in the same way from the random observers results as **LGO**-ones. As we have already noticed, for all three estimators the scatter connected with a LG-like observer is much larger than for the random observer sample. We have checked that sampling variance is not contributing significantly to this scatter, as all estimates are based on comparable pair-number counts per bin. This implies that even for the signal extracted at large galaxy pair separations, the variance induced by the local structures is large and significant. This is an intrinsic LG-like observer property and as such for a realistic case of one LG-

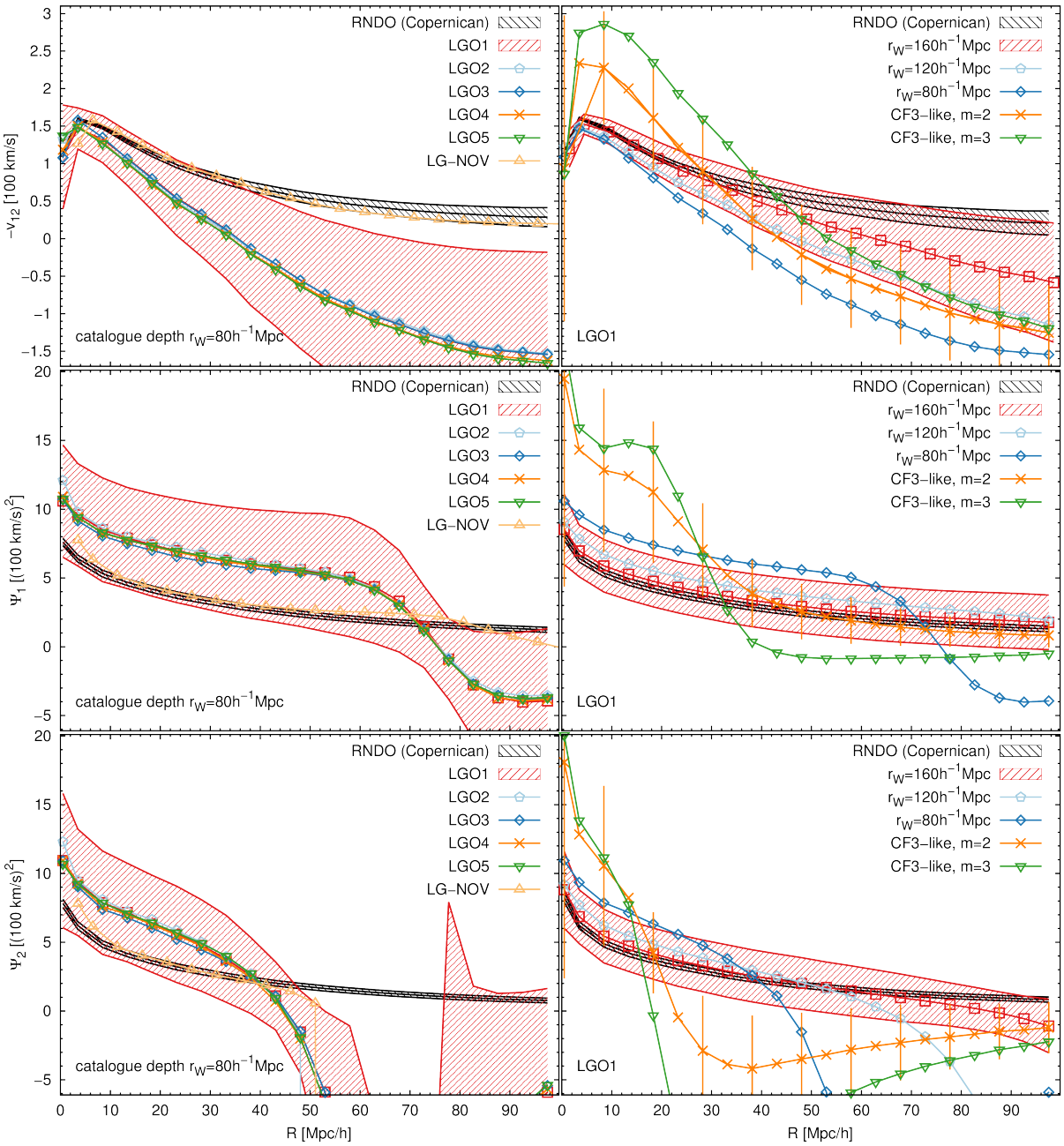


**Figure 3.** The effects of **LGO**-like observer location and various selection functions on the velocity statistics. Error-bars and filled regions mark $1\sigma$ observer-to-observer scatter around ensemble mean. From to to bottom panels show results for $v_{12}$, $\psi_1$ and $\psi_2$ respectively. The left column illustrate the effects for different set of observers, but with the same imposed radial selection cut of $r_w = 80h^{-1}\,\mathrm{Mpc}$. The right column of panels focuses on our main Local Group (**LGO1**) observers sample and the comparison of various selection functions and data weights.

observer, this large scatter will manifest *as a systematic error* on the velocity correlation functions.

The column to the right of Fig. 3 shows the same statistics obtained for one and the same main **LGO1** list, but with both data weighting schemes considered. For the simplistic scheme of Eqn. (17) we implement the following catalogue depths: $r_w = 80, 120, 160h^{-1}\,\mathrm{Mpc}$. In addition we also consider two CF3-like samples with $m = 2$ and $m = 3$. The right column of panels in Fig. 3 shows how the effective radial depth and related incompleteness affects $v_{12}, \psi_1$ and $\psi_2$. The behaviour of curves corresponding to different radial selection cuts is qualitatively similar for all three panels. As expected, the shallower the catalogue, the bigger the effect of observer location. For CF3-like selection functions the effects of the observer's location become more severe for $R \lesssim 40h^{-1}\,\mathrm{Mpc}$, where both the scatter and the relative differences are bigger than for the shallowest $r_w = 80h^{-1}\,\mathrm{Mpc}$ **LGO**-case. Yet, at larger pair separations it seems that the situation is partially remedied, where (especially for $m = 2$) the data from more distant galaxies bring the curves again closer to **RNDO**. In contrast to the situation we have encountered for a simple $r_w = 80h^{-1}\,\mathrm{Mpc}$ cuts presented in the left panels, where $\psi_2$ appeared as the least affected statistics, here for a CF3-like selection function, it is $\psi_1$ that is char-

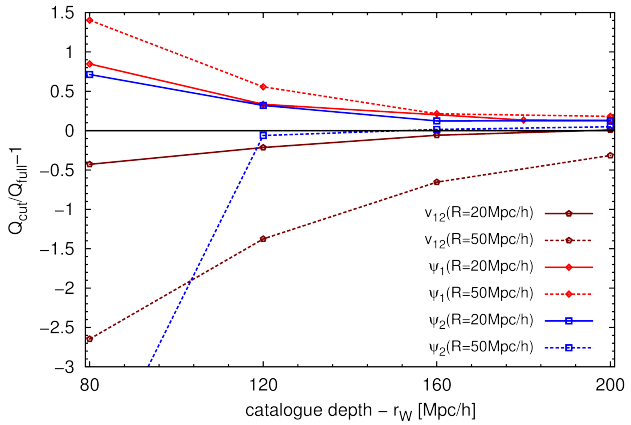


**Figure 4.** The biasing of the LG observer estimators with respect to a Copernican observer as a function of the velocity catalogue depth parameter, $r_w$. The ratios for each estimator are taken at two pair separation scales: $20h^{-1}$ Mpc and $50h^{-1}$ Mpc.

acterised by least biased behaviour. For $R \geqslant 40h^{-1}$ Mpc its average is even consistent within $1\sigma$ with the Copernican observer's one. Finally, as one might expect the difference between random observers and the deepest $r_w = 160h^{-1}$ Mpc **LGO1** catalogue are very small (when compared to differences visible for shallower catalogues).

To allow for a better assessment of the effect on the velocity statistics inferred by **LGO1** observers, we plot in Fig. 4 the ratio of LG-based estimators with respect to Copernican observers as a function of the catalogue depth parameter $r_w$. We focus on ratios taken at two pair separations of 20 and $50h^{-1}$ Mpc. We also add a catalogue with $r_w = 200h^{-1}$ Mpc, which benchmarks the limiting case of an idealized very deep velocity survey. It is clear now that both $r_w = 80h^{-1}$ Mpc and $120h^{-1}$ Mpc samples are dramatically affected by the limited depth of their halo catalogues. For $80h^{-1}$ Mpc depth catalogue the differences from the full depth one can be typically as large as $> 4\sigma$, while for $120h^{-1}$ Mpc catalogue the deviations from the unbiased case are contained in the range of $2 - 2.5\sigma$. The situation is better for the two deepest catalogues we consider with cuts at 160 and $200h^{-1}$ Mpc. However, here, even for $200h^{-1}$ Mpc case the differences between values inferred from a realistic catalogue and an "idealized" deep one are bigger than $1\sigma$ for $R \gtrsim 50h^{-1}$ Mpc in $v_{12}$ case, and $R \gtrsim 20h^{-1}$ Mpc for $\psi_1$. For $r_w \geqslant 120h^{-1}$ Mpc and $R \geqslant 50h^{-1}$ Mpc the results for the $\psi_2$-estimator seems to be the closest one to universal cosmic mean of **RNDO**. We caution however, that as indicated by the results shown in the bottom-right panel of Fig. 3 for a more realistic CF3-like selection functions, $\psi_2$ at those large separations is more affected than $\psi_1$. In all cases the scatter due to observer location induced by limited depth of catalogues is large, and as expected grows with shrinking catalogue depth.

## 6 DISCUSSION AND CONCLUSIONS

In this paper we considered the estimation of two-point peculiar velocity statistics. We have refrained from assessing important effects related to observational errors such as Malmquist biases, and focused on the impact of cosmic variance and observer location.

We have tested the ability of the radial velocity based estimators in Eqns. (7), (8) and (16) at recovering the underlying correlations in the case of of complete coverage velocity catalogues. The $v_{12}$ estimator of Ferreira et al. (1999) performs very well by measuring the averaged infall velocity with a percent-level accuracy. The theoretical predictions for both correlations functions were off by a factor of $8 - 16\%$. Thus, even for perfect data the measured values of $\psi_1$ and $\psi_2$ should be compared with theoretical predictions of Eqn. (9) with care. Further, since for realistic data these statistics depend strongly on the data completeness, a much better approach is to derive predictions for both Górski et al. (1989) functions based on realistic mock catalogues, rather than a simplistic relation as the one expressed by Eqns. (4), (5) and (9).

Next we have checked if a sampling bias due to strong undersampling would be an issue. This was a relevant test, as the currently available galaxy peculiar velocity catalogues contain a relatively small number ($\sim 10^4$) of objects. The tests show that all three velocity statistics are not sensitive to under-sampling. The ensemble averages of 10% and 1%-sub-samples (with effective $\bar{n} = 9 \times 10^{-4}$ and $9 \times 10^{-5}\, h^3\mathrm{Mpc}^{-3}$ number densities) were statistically consistent with the full sample. Only in the case of a severe sub-sampling of the 0.1%-case (with $\bar{n} = 9 \times 10^{-6}\, h^3\mathrm{Mpc}^{-3}$) the estimated mean showed some noticeable scatter around the true mean. In addition, we have found that the scatter around the mean is scale dependent, being a strong function of a pair separation for $v_{12}$. Albeit for both $\psi$'s, except the smallest scales of $R < 30h^{-1}$ Mpc, the scatter shows only a very weak evolution with scale. All in all, we can report that all the three studied velocity statistics are performing well in the sparse sampling regime.

Our most important result is related to the effect of the observed large scale environment on velocity statistics. We have performed a detailed analysis of cosmic variance in velocity statistics by considering differences in velocity observables as measured by a Copernican observer and LG-equivalents. We have considered four criteria compatible with LG properties and local environment. Velocity two-point statistics are found to be insensitive to the criteria related to the MW halo mass and the LG motion and its mean density (within $\sim 3h^{-1}$ Mpc). In contrast, the proximity of an observer to a Virgo-like cluster is highly significant, affecting the correlations up to scales of $\sim 100h^{-1}$ Mpc. This has not been noticed by Tormen et al. (1993) since they only consider LG-analogue observers defined without imposing the presence of a nearby massive cluster.

In the near future, peculiar velocity surveys are not likely to reach to much larger distances than currently, although the number densities will be growing. For instance, *CosmicFlows-4* is expected to contain of the order of $3 \times 10^4$ sources but still mostly within $R < 150h^{-1}$ Mpc as currently CosmicFlows-3 does[3]. It is only the advent of all-sky HI radio surveys that can extend the reach of PV surveys to $\sim 2$ times larger distances, and the object number closer to $10^5$.

Careful modelling of observer location, and survey selection strategy are necessary for obtaining reliable and unbiased velocity correlation estimates. Much more effort is required to extract cosmological information richly stored in galaxy velocity data. Towards this goal, constrained realization techniques (Hoffman & Ribak 1991; van de Weygaert & Bertschinger 1996; Klypin et al. 2003; Courtois & Tully 2012; Heß et al. 2013; Sorce et al. 2016), aiming at incorporating prominent structures in the real Universe can be very rewarding.

[3] Tully, private communication.

## ACKNOWLEDGEMENTS

The Authors have benefited from many inspiring discussions with Hélène Courtois, Noam Libeskind and Brent Tully. The hospitality of the Technion – Israel Institute of Technology enjoyed by WAH,MF and MB at the early stages of this project is warmly acknowledged. WAH acknowledges support from European Research Council (grant number 646702 "CosTesGrav"). WAH and MB were also supported by the Polish National Science Center under contract #UMO-2012/07/D/ST9/02785. This research was supported by the I-CORE Program of the Planning and Budgeting Committee, THE ISRAEL SCIENCE FOUNDATION (grants No. 1829/12 and No. 203/09) and the Asher Space Research Institute. MF acknowledges support through the Grant Spin(e) ANR-13-BS05-0005 of the French National Research Agency.

## REFERENCES

Alpaslan M., et al., 2014, MNRAS, 438, 177
Behroozi P. S., Wechsler R. H., Wu H.-Y., 2013, ApJ, 762, 109
Berti E., et al., 2015, Classical and Quantum Gravity, 32, 243001
Bilicki M., Chodorowski M. J., 2010, MNRAS, 406, 1358
Borgani S., da Costa L. N., Zehavi I., Giovanelli R., Haynes M. P., Freudling W., Wegner G., Salzer J. J., 2000, AJ, 119, 102
Bull P., 2016, ApJ, 817, 26
Busha M. T., Wechsler R. H., Behroozi P. S., Gerke B. F., Klypin A. A., Primack J. R., 2011, ApJ, 743, 117
Cautun M. C., van de Weygaert R., 2011, preprint, (arXiv:1105.0370)
Cautun M., Frenk C. S., van de Weygaert R., Hellwing W. A., Jones B. J. T., 2014, MNRAS, 445, 2049
Chodorowski M. J., Ciecielag P., 2002, MNRAS, 331, 133
Colless M., et al., 2001, MNRAS, 328, 1039
Cooray A., Caldwell R. R., 2006, Phys. Rev. D, 73, 103002
Courtois H. M., Tully R. B., 2012, Astronomische Nachrichten, 333, 436
Courtois H. M., Tully R. B., Makarov D. I., Mitronova S., Koribalski B., Karachentsev I. D., Fisher J. R., 2011, MNRAS, 414, 2005
Courtois H. M., Pomarède D., Tully R. B., Hoffman Y., Courtois D., 2013, AJ, 146, 69
Davis M., Peebles P. J. E., 1977, ApJS, 34, 425
Davis M., Nusser A., Masters K. L., Springob C., Huchra J. P., Lemson G., 2011, MNRAS, 413, 2906
Elyiv A. A., Karachentsev I. D., Karachentseva V. E., Melnyk O. V., Makarov D. I., 2013, Astrophysical Bulletin, 68, 1
Fagernes Ivarsen M., Bull P., Llinares C., Mota D. F., 2016, preprint, (arXiv:1603.03072)
Feix M., Nusser A., Branchini E., 2015, Physical Review Letters, 115, 011301
Feldman H., et al., 2003a, ApJ, 596, L131
Feldman H., et al., 2003b, ApJ, 596, L131
Ferreira P. G., Juszkiewicz R., Feldman H. A., Davis M., Jaffe A. H., 1999, ApJ, 515, L1
Geller M. J., Huchra J. P., 1989, Science, 246, 897
Górski K., 1988, ApJ, 332, L7
Górski K. M., Davis M., Strauss M. A., White S. D. M., Yahil A., 1989, ApJ, 344, 1
Groth E. J., Juszkiewicz R., Ostriker J. P., 1989, ApJ, 346, 558
Gudehus D., 1995, A&A, 302, 21
Guo Q., Cooper A. P., Frenk C., Helly J., Hellwing W. A., 2015, MNRAS, 454, 550
Guzzo L., et al., 2014, A&A, 566, A108
Hellwing W. A., 2014, preprint, (arXiv:1412.8738)
Hellwing W. A., Barreira A., Frenk C. S., Li B., Cole S., 2014, Physical Review Letters, 112, 221102
Hellwing W. A., Schaller M., Frenk C. S., Theuns T., Schaye J., Bower R. G., Crain R. A., 2016, MNRAS, 461, L11
Heß S., Kitaura F.-S., Gottlöber S., 2013, MNRAS, 435, 2065
Hinshaw G., et al., 2013, ApJS, 208, 19
Hoffman Y., Ribak E., 1991, ApJ, 380, L5
Huchra J., Davis M., Latham D., Tonry J., 1983, ApJS, 52, 89
Hudson M. J., 1993, MNRAS, 265, 43
Hudson M. J., Turnbull S. J., 2012, ApJ, 751, L30
Juszkiewicz R., Springel V., Durrer R., 1999, ApJ, 518, L25
Juszkiewicz R., Ferreira P. G., Feldman H. A., Jaffe A. H., Davis M., 2000, Science, 287, 109
Karachentsev I. D., et al., 2002, A&A, 389, 812
Karachentsev I. D., et al., 2003, A&A, 398, 479
Karachentsev I. D., Karachentseva V. E., Melnyk O. V., Elyiv A. A., Makarov D. I., 2012, Astrophysical Bulletin, 67, 353
Karachentsev I. D., Tully R. B., Wu P.-F., Shaya E. J., Dolphin A. E., 2014, ApJ, 782, 4
Klypin A., Hoffman Y., Kravtsov A. V., Gottlöber S., 2003, ApJ, 596, 19
Kogut A., et al., 1993, ApJ, 419, 1
Komatsu E., et al. 2010, preprint, (arXiv:1001.4538)
Li B., Hellwing W. A., Koyama K., Zhao G.-B., Jennings E., Baugh C. M., 2013, MNRAS, 428, 743
Lu N. Y., Salpeter E. E., Hoffman G. L., 1994, ApJ, 426, 473
Lynden-Bell D., Burstein D., Davies R. L., Dressler A., Faber S. M., 1988a, in van den Bergh S., Pritchet C. J., eds, Astronomical Society of the Pacific Conference Series Vol. 4, The Extragalactic Distance Scale. pp 307–316
Lynden-Bell D., Faber S. M., Burstein D., Davies R. L., Dressler A., Terlevich R. J., Wegner G., 1988b, ApJ, 326, 19
Ma Y.-Z., Li M., He P., 2015, A&A, 583, A52
Marra V., Amendola L., Sawicki I., Valkenburg W., 2013, Physical Review Letters, 110, 241305
Mei S., et al., 2007, ApJ, 655, 144
Milne E. A., 1935, Relativity, gravitation and world-structure
Nadathur S., 2013, MNRAS, 434, 398
Nusser A., Colberg J. M., 1998, MNRAS, 294, 457
Nusser A., Lahav O., 2000, MNRAS, 313, L39
Nusser A., Branchini E., Davis M., 2011, ApJ, 735, 77
Nusser A., Branchini E., Davis M., 2012, ApJ, 755, 58
Peebles P. J. E., 1980, The large-scale structure of the universe. Research supported by the National Science Foundation. Princeton, N.J., Princeton University Press, 1980. 435 p.
Phelps S., Nusser A., Desjacques V., 2013, ApJ, 775, 102
Planck Collaboration et al., 2015, preprint, (arXiv:1502.01589)
Sánchez A. G., et al., 2012, MNRAS, 425, 415
Sandage A., 1978, AJ, 83, 904
Sandage A., Tammann G. A., Hardy E., 1972, ApJ, 172, 253
Sarkar D., Feldman H. A., Watkins R., 2007, MNRAS, 375, 691
Schaap W. E., van de Weygaert R., 2000, A&A, 363, L29
Schaye J., et al., 2015, MNRAS, 446, 521
Schlegel D., Davis M., Summers F., Holtzman J. A., 1994, ApJ, 427, 527
Scrimgeour M. I., et al., 2012, MNRAS, 425, 116
Soifer B. T., et al., 1984, ApJ, 278, L71
Sorce J. G., et al., 2016, MNRAS, 455, 2078
Springel V., 2005, MNRAS, 364, 1105
Springob C. M., Masters K. L., Haynes M. P., Giovanelli R., Marinoni C., 2007, ApJS, 172, 599
Springob C. M., et al., 2014, MNRAS, 445, 2677
Strauss M. A., Willick J. A., 1995, Phys. Rep., 261, 271
Strauss M. A., Ostriker J. P., Cen R., 1998, ApJ, 494, 20
Tammann G. A., Sandage A., 1985, ApJ, 294, 81
Tegmark M., et al., 2004, Phys. Rev. D, 69, 103501
The Planck Collaboration et al., 2013, preprint, (arXiv:1303.5076)
Tormen G., Moscardini L., Lucchin F., Matarrese S., 1993, ApJ, 411, 16
Tully R. B., Fisher J. R., 1987, Atlas of Nearby Galaxies
Tully R. B., Fisher J. R., 1988, Catalog of Nearby Galaxies
Tully R. B., Shaya E. J., 1984, ApJ, 281, 31
Tully R. B., Shaya E. J., Karachentsev I. D., Courtois H. M., Kocevski D. D., Rizzi L., Peel A., 2008, ApJ, 676, 184
Tully R. B., et al., 2013, AJ, 146, 86
Tully R. B., Courtois H., Hoffman Y., Pomarède D., 2014, Nature, 513, 71

Tully R. B., Courtois H. M., Sorce J. G., 2016, preprint, (arXiv:1605.01765)
Uzan J.-P., 2009, Space Sci. Rev., 148, 249
Vittorio N., Juszkiewicz R., Davis M., 1986, Nature, 323, 132
Wojtak R., Knebe A., Watson W. A., Iliev I. T., Heß S., Rapetti D., Yepes G., Gottlöber S., 2014, MNRAS, 438, 1805
Zel'Dovich Y. B., 1970, A&A, 5, 84
Zu Y., Weinberg D. H., Jennings E., Li B., Wyman M., 2013, preprint, (arXiv:1310.6768)
van de Weygaert R., Bertschinger E., 1996, MNRAS, 281, 84
van de Weygaert R., Schaap W., 2009, in Martínez V. J., Saar E., Martínez-González E., Pons-Bordería M.-J., eds, Lecture Notes in Physics, Berlin Springer Verlag Vol. 665, Data Analysis in Cosmology. pp 291–413, doi:10.1007/978-3-540-44767-2˙11

This paper has been typeset from a TEX/LATEX file prepared by the author.